Blanchy, G., Watts, C. W., Richards, J., Bussell, J., Huntenburg, K., Sparkes, D. L., Stalham, M., Hawkesford, M. J., Whalley, W. R. and Binley, A. 2020. Time-lapse geophysical assessment of agricultural practices on soil moisture dynamics. *Vadose Zone Journal.* 19 (1), p. e20080. https://doi.org/10.1002/vzj2.20080

Received: 15 July 2020 | Accepted: 28 September 2020

DOI: 10.1002/vzj2.20080

Vadose Zone Journal

SPECIAL SECTION: AGROGEOPHYSICS: GEOPHYSICS TO INVESTIGATE SOIL–PLANT–ATMOSPHERE INTERACTIONS & SUPPORT AGRICULTURAL MANAGEMENT

Time-lapse geophysical assessment of agricultural practices on soil moisture dynamics

Guillaume Blanchy[1,2] | Chris. W. Watts[2] | Jake Richards[3] | Jennifer Bussell[3,4] | Katharina Huntenburg[1] | Debbie L. Sparkes[3] | Mark Stalham[5] | Malcolm J. Hawkesford[2] | W. Richard Whalley[2] | Andrew Binley[1]

[1] Lancaster Univ., Lancaster, Lancashire LA1 4YW, UK

[2] Rothamsted Research, Harpenden, Hertfordshire AL5 2JQ, UK

[3] Univ. of Nottingham, Nottingham, Nottinghamshire NG7 2RD, UK

[4] The Game & Wildlife Conservation Trust, Allerton Project, Loddington, Leicestershire LE7 9XE, UK

[5] NIAB CUF, Cambridge, Cambridgeshire CB3 0DL, UK

Correspondence

Guillaume Blanchy, Lancaster Univ., Lancaster, Lancashire, LA1 4YW, UK.
Email: g.blanchy@lancaster.ac.uk

Assigned to Associate Editor Benjamin Mary.

Funding information

Biotechnology and Biological Sciences Research Council, Grant/Award Numbers: BB/J004286/1, BB/P016855/1, BBS/E/C/00I0330; AHDB-Lancaster, Grant/Award Numbers: 110002102, &, 110002104

Abstract

Geophysical surveys are now commonly used in agriculture for mapping applications. High-throughput collection of geophysical properties such as electrical conductivity (inverse of resistivity) can be used as a proxy for soil properties of interest (e.g., moisture, texture, salinity). Most applications only rely on a single geophysical survey at a given time. However, time-lapse geophysical surveys have greater capabilities to characterize the dynamics of the system, which is the focus of this work. Assessing the impact of agricultural practices through the growth season can reveal important information for the crop production. In this work, we demonstrate the use of time-lapse electrical resistivity tomography (ERT) and electromagnetic induction (EMI) surveys through a series of three case studies illustrating common agricultural practices (cover crops, compaction with irrigation, and tillage with N fertilization). In the first case study, time-lapse EMI reveals the initial effect of cover crops on soil drying and the absence of effect on the subsequent main crop. In the second case study, compaction leading to a shallower drying depth for potatoes (*Solanum tuberosum* L.) was imaged by time-lapse ERT. In the third case study, larger changes in electrical conductivity over time were observed in conventional tillage compared with direct drill using time-lapse EMI. In addition, different N application rates had a significant effect on the yield and leaf area index but only ephemeral effects on the dynamics of electrical conductivity, mainly after the first application. Overall, time-lapse geophysical surveys show great potential for monitoring the impact of different agricultural practices that can influence crop yield.

Abbreviations: EC, electrical conductivity; ECa, apparent electrical conductivity; EMI, electromagnetic induction; ERT, electrical resistivity tomography; LAI, leaf area index.

1 | INTRODUCTION

Geophysical methods such as electromagnetic induction (EMI) and electrical resistivity tomography (ERT) are increasingly being used for agricultural applications.

Electrical resistivity tomography enables the generation of an image of the electrical resistivity of the subsurface from measurements made using electrodes in contact with the ground. In contrast, EMI senses the electrical conductivity (EC, the inverse of resistivity) of the ground through inductive signals and thus does not require galvanic contact with the subsurface. Originating in part from the mineral and oil exploration industries (Schlumberger, 1920), ERT is now widely used for many shallow near-surface applications. Electromagnetic induction has proved effective for soil salinity mapping (Corwin & Lesch, 2005). It has since been widely used for mapping different soil properties (Doolittle & Brevik, 2014), defining management zones in agriculture (Hedley, Yule, Eastwood, Shepherd, & Arnold, 2004), or assessing soil structure (Romero-Ruiz, Linde, Keller, & Or, 2018). More recently the development of multi-coil EMI instruments has enabled simultaneous measurements at multiple depths, enabling the recovery of the distribution of EC of the subsurface as in ERT.

Understanding the availability and movement of water in the ground has become a significant driver for many geophysical studies and has led to the field of hydrogeophysics (Binley et al., 2015). Geophysical methods have the capability to characterize properties of soil that influence the flow and storage of soil water, making such methods relevant for plant-related application (Cimpoiaşu, Kuras, Pridmore, & Mooney, 2020; Jayawickreme, Jobbágy, & Jackson, 2014; Shanahan, Binley, Whalley, & Watts, 2015; Whalley et al., 2017; Zhao et al., 2019). For more information on other geophysical methods, we redirect the reader to the review of Allred et al. (2008), who illustrate a range of geophysical applications in agriculture, and the broader overview of geophysical methods for proximal soil sensing given by Viscarra Rossel, Adamchuk, Sudduth, McKenzie, and Lobsey (2011). These reviews focus on static surveys for assessment of soil properties and states; however, there is much greater potential for geophysical methods for characterizing the dynamic state of the subsurface, which is the focus of this study.

Soil and water are essential resources for agriculture. However, these resources are endangered by intensive agricultural practices that can affect food security (Amundson et al., 2015). Loss of soil structure due to tillage or compaction can substantially affect the plant water availability and nutrient uptake and affect crop growth. Conservation agriculture practices aim at addressing some of these specific issues and improve and sustain crop production. The FAO (http://www.fao.org/conservation-agriculture/en/) defines three axes for conservation agriculture: (1) minimum mechanical soil disturbance, (2) permanent soil organic cover, and (3) species diversification. The case studies presented in this work concentrates on Axes 1 and 2. More specifically, this paper focuses on the agricultural practices: compaction with irrigation, tillage with N fertilization, and cover crops. This work does not aim at exhaustively detailing each practice but rather at assessing the potential of two popular geophysical methods (ERT and EMI) at monitoring the effects of these different management practices on soil properties and soil water status.

Core Ideas

- Time-lapse geophysical surveys can help assess the impact of agricultural practices.
- Cover crops affect soil drying while in place but have no substantial effect on the main crop.
- Traffic-induced soil compaction limits water extraction depths of potato crops.
- The soil electrical conductivity in moldboard plowing decreases faster than in direct drill.
- N levels have significant impact on the soil EC after application, but not over a longer term.

Traffic-induced soil compaction can be significant in certain (mainly loamy) soils as the compaction occurs in deeper layers. Over short time scales, compaction reduces the soil porosity, making it more difficult for the roots to penetrate and the water to circulate in the soil (Keller et al., 2013), potentially affecting the effectiveness of irrigation practices. We redirect the reader to Hamza and Anderson (2005) and Batey (2009) who review the different agricultural impacts of soil compaction. Soil compaction can also have long-term effects (Keller et al., 2017).

Tillage, conventionally moldboard plowing, increases the soil porosity but worsens the soil structure. Direct drilling (zero-tillage) offers an alternative to conventional tillage, as it prevents major disruption of the soil structure. The structure of the soil plays a key role in making water and nutrients available to the crop and hence can affect crop productivity. Although tillage has other major implications for the biological activity of the soil (Hobbs, Sayre, & Gupta, 2008), the case study presented in this manuscript focuses on the comparison of plowing and direct drill treatments on the soil moisture dynamics and N uptake.

Cover crops, usually sown in a sequence with the main cash crop, have many benefits. They can improve the soil structure, increase the availability of organic matter, and also prevent the loss of nutrients to depth, among other advantages (Fageria, Baligar, & Bailey, 2005). Deep-rooting cover crops can increase the porosity of the soil, hence potentially improving the water availability for the main crop.

The impact of these practices on the agricultural ecosystem is often assessed using small sampling volumes over a short time window. Some methods, such as soil coring or installation of access tubes for soil moisture probes, can be destructive for the crop and the soil. In contrast, geophysical methods such as ERT and EMI are minimally invasive and enable repeated measurements without disturbing the growth of the crop. The other significant advantages of geophysical methods are their large sampling volume and their high-throughput data collection, making them well suited to study field-scale processes.

All these advantages make geophysical methods attractive for obtaining a quick, single-scan survey of the field. This single mapping approach is widely used today and even commercially available for obtaining a proxy textural map for precision agriculture. However, such an approach is not well suited to study highly dynamic soil–plant–water interactions. Instead of a single survey, we argue that geophysical time-lapse monitoring can bring more information about how the agricultural practices influence the soil–plant–water interactions and how this can affect crop productivity.

Through a series of case studies, this manuscript aims to demonstrate the potential of time-lapse geophysical investigation to better understand the impact of these practices on the soil moisture dynamics. Specifically, the manuscript aims (a) to highlight the potential of time-lapse geophysical surveys to assess conservation agricultural practices; (b) to detail the current limitations of the approach; and (c) to provide recommendations on the use of time-lapse geophysical monitoring.

2 | MATERIALS AND METHODS

2.1 | Geophysical properties

Geophysical methods measure geophysical properties, which are then linked to soil properties of interest using pedophysical relationships (Archie, 1942; Boaga, 2017; Laloy, Javaux, Vanclooster, Roisin, & Bielders, 2011; Rhoades, Raats, & Prather, 1976; Waxman & Smits, 1968; Wunderlich, Petersen, Attia al Hagrey, & Rabbel, 2013). Electrical resistivity tomography measures the soil electrical resistivity using galvanic coupling and EMI measures the soil EC using inductive coupling. The soil EC (or resistivity) is influenced by many factors such as soil temperature, soil moisture, pore water EC, soil texture, and porosity. This makes the interpretation of EC values challenging, as the user needs to identify the dominant factor influencing EC for a given site and account for the effect of the other factors. This also emphasizes the need for site-specific relationships (Calamita, Perrone, Brocca, Onorati, & Manfreda, 2015).

The time-lapse approach can help here, as some factors are usually relatively constant during the survey time, such as soil texture and porosity. Soil temperature can be corrected for (Ma, McBratney, Whelan, Minasny, & Short, 2011), and in a nonsaline rainfed environment, the EC of the pore water can often be assumed to remain constant except when fertilizers or other chemicals are applied. Thus, the soil moisture is often the main factor controlling the change in EC observed over the growing season of a crop.

2.2 | Electrical resistivity tomography

Electrical resistivity tomography uses multiple electrodes to measure the distribution of the electrical resistivity of the subsurface. In the case studies of this manuscript, all electrodes are located on the surface, but other configuration might involve borehole electrodes, hence increasing the sensitivity of the measurements at depth. The ERT measurements are made using four electrodes: a quadrupole. Current is injected between two electrodes, and the difference in electrical potential is measured between the other two. Each measurement provides an apparent resistivity (i.e., the resistivity of an equivalent homogeneous subsurface). Given multiple combinations of current and potential electrodes along a transect, a two-dimensional image of the true resistivity can be reconstructed using inverse modeling (Binley, 2015). For a more detailed review on ERT methods in soil science, the reader is directed to Samouëlian, Cousin, Tabbagh, Bruand, and Richard (2005).

2.3 | Electromagnetic induction

Electromagnetic induction instruments use EMI principles to measure the apparent EC (ECa) of the subsurface. By making measurements with different induction coil spacing and/or orientation, it is possible to sense different depths of the subsurface, and thus like ERT, inverse methods can be used to convert the apparent conductivity measurements to a depth profile of EC (McLachlan, Blanchy, & Binley, 2020; von Hebel et al., 2019). The instrument used in this study is the CMD Mini-Explorer (GF Instruments), which is composed of one transmitter coil and three receiver coils and can be used in horizontal co-planar (HCP) or vertical co-planar (VCP) orientation. When measuring, the transmitter coil emits a primary time-varying electromagnetic field that induces eddy currents proportional to the ground EC. These eddy currents, in turn, induce a secondary electromagnetic field. Both primary and secondary electromagnetic fields are sensed by the receiver coils. From their ratio, a depth-weighted ECa can be derived. The larger the separation between the transmitter and the receiver coil, the deeper the volume investigated. The combination of HCP–VCP orientations and the three coils separations enables the collection of up to six data points per sampling location with the CMD Mini-Explorer. In the rest of the manuscript coil configuration will be presented as VCP0.32 with VCP the orientation and 0.32 the coil separation in meters. We redirect the reader to Callegary, Ferré, and Groom (2007) for more information on the specific aspects of EMI measurements. The inverted change in EC profiles presented in this manuscript were obtained using a Gauss–Newton approach following Whalley et al. (2017), implemented in the open-source code EMagPy (McLachlan et al., 2020).

The ECa maps provided by the EMI instruments are often qualitative, showing areas of higher EC and lower EC. Although this does not have any impact for mapping applications, its effect is significant for quantitative application. Different methods exist to calibrate apparent EMI values based on independently measured depth profiles of EC. Trenches and soil samples can be used to build an EC depth profile. In this study, EMI calibration was done using the inverted EC values from an ERT transect (Lavoué et al., 2010; von Hebel et al., 2014). Other methods such as using multi-elevation measurements have also been proposed to calibrate EMI data (Tan et al., 2019). von Hebel et al. (2019) reviewed the best practices for calibration, conversion, and inversion of EMI data.

2.4 | Time-lapse approach

A one-time geophysical survey is useful for assessing the static soil properties, but when assessing dynamic states such as soil moisture, the time-lapse approach is more appropriate. The time-lapse approach consists of multiple surveys taken at different times during the period of interest (e.g., the growing season of a crop). A reference survey, usually chosen as a "wet" or "dry" reference, is subtracted from the other surveys to obtain a change in EC. This way, static effects on soil EC (e.g., from texture) are accounted for and only the dynamic part of the EC is analyzed. In non-arid conditions, one of the major drivers of the change in EC observed through the season is the change in soil moisture. Since rainfall events can induce sudden increases in soil moisture, when surveys are focused on assessing changes due to evapotranspiration, field measurements should be conducted after significant rainfall events to avoid sensing localized changes in soil moisture.

Note that the EC (and hence resistivity) is sensitive to temperature and hence a temperature correction is needed for proper interpretation of a time-lapse survey (Hayashi, 2004; Ma et al., 2011). In this study, ECa values were corrected using

$$EC_{25} = \frac{EC_T}{1 + 0.02\,(T - 25)} \quad (1)$$

where EC_{25} is the temperature corrected EC (at 25 °C), and T is the soil temperature (°C). When soil temperature profiles were available (all studies except the compaction case), a depth-weighted temperature was computed using the cumulative sensitivity function of the EMI instrument (Blanchy, Watts, et al., 2020). This "apparent" temperature was then used in Equation 1 to correct the ECa values.

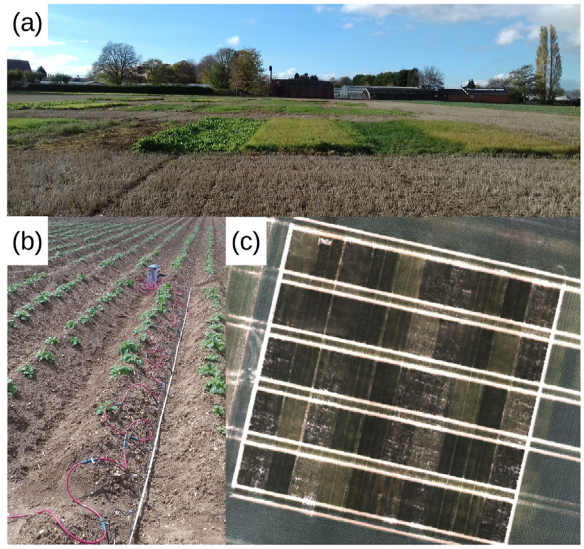

FIGURE 1 (a) Long-term cover crop experiment (picture taken on 9 Oct. 2018). (b) Compaction experiment on potatoes showing an electrical resistivity tomography (ERT) measurement taking place in a furrow. (c) Experiment on the effects of tillage and nitrogen treatment on winter wheat

2.5 | Experiments

To demonstrate the potential of time-lapse geophysics to study the impact of different agricultural practices, three case studies with different crops were selected (Figure 1). The first one focuses on the impact of cover crops on the soil moisture availability for the main crop (sugar beet, *Beta vulgaris* L). It also compares short-term and long-term cover crops (Figure 1a). The second case focuses on the impact of soil compaction with two different irrigation treatments on the water uptake of potatoes (Figure 1b). The third case explores the interactions between two types of tillage (moldboard plowing and direct drill) and different application rates of N fertilizer on winter wheat (*Triticum aestivum* L.; Figure 1c).

2.5.1 | Cover crops

Two experiments were carried out with cover crops aiming at assessing the impact on the cover crops on soil moisture availability for the main crop. Cover crops are usually sown in autumn after the harvest of the main crop. They are kept over the winter and, if needed, are destroyed in spring before sowing of the main crop. The hypothesis behind these experiments is that cover crops will improve the soil structure via its root system. The improved soil structure will then help the following cash crop (in this case, sugar beet) to better access soil moisture. Time-lapse EMI was used to monitor the potential effect of the cover crops on the dynamics of soil moisture.

The first experiment was sown with the different cover crops in September 2016 at Nottingham Sutton Bonington campus (52°50′12.4“ N, 1°15′05.7″ W) on a Cambisol (World Reference Base) with a texture of 13.2% clay, 19.5% silt, and 67.3% sand. The cover crops were sown in a random block design of four blocks with eight plots (3 × 7.5 m) per block. Seven different cover crops were tested: oil radish (*Raphanus sativus* L.), tillage radish (*Raphanus sativus* L.), forage rye (*Secale cereale* L.), black oat (*Avena strigosa* Schreb.), white mustard (*Sinapsis alba* L.), and Egyptian clover (*Trifolium alexandrinum* L.). An additional bare soil plot was also part of the treatments as a reference. The cover crops were destroyed in December 2016. Sugar beet was then established using direct drilling in spring of the following year and harvested in autumn. The EMI data were collected using the CMD Mini-Explorer (GF Instruments) on 9 Nov. 2016, 8 Dec. 2016 (a few days after the crop was destroyed), 8 Mar. 2017, 11 May 2017, and 22 June 2017.

The second experiment was sown with cover crops in September 2017 in a field near to the first experiment (52°49′53.8“ N 1°14′49.3″ W), also classified as a Cambisol. Its aim was not only to estimate the impact of cover crops on soil moisture availability but also to compare cover crops grown over the winter with cover crops in place for a full season. The experimental design was composed of four blocks with 10 plots per block (12 × 3 m). Four different cover crops were tested: chicory (*Cichorium intybus* L.), a mix of red clover (*Trifolium repens* L.) and cocksfoot (*Dactylis* spp L.), lucerne (also called alfalfa; *Medicago sativa* L.), and cocksfoot alone. An additional bare soil treatment was also added as a reference. In September 2017, the five cover crop treatments were applied to five plots inside each block. Wheat was grown on the unattributed plots. In September 2018, after the wheat had been harvested, the five treatments were applied on the remaining plots. As such, each block contained two plots with the same treatment, but one was in place since September 2017 and one was in place since September 2018. Figure 1a shows the experiment in October 2018. At the beginning of March 2019, the cover crops were destroyed, and sugar beet was sown using direct drilling. Sugar beet was harvested in autumn 2019. The EMI data were collected on 25 Oct. 2017, 8 Dec. 2017, 26 Mar. 2018, 19 June 2018, 1 Aug. 2018, 29 Oct. 2018, 11 Mar. 2019, 14 May 2019, 4 June 2019, 3 July 2019, and 10 Sept. 2019. The EMI data were calibrated using ERT lines collected in another experiment nearby following Lavoué et al. (2010).

2.5.2 | Compaction and irrigation

A compacted soil can potentially impede root water extraction and hence lead to water stress for some crops. In this experiment, the impact of soil compaction and irrigation is explored on potatoes. The compaction experiment took place in a field managed by the NIAB Agronomy Centre (52°14′13.4“ N 0°05′57.9″ E) in Cambridge, UK, in 2018. Two different treatments were applied: compaction or no compaction, and frequent irrigation (wet) or severe deficit irrigation (dry). The experiment was composed of four replicate blocks (16 plots, each 3 × 4.5 m) planted with potato cultivar ‘Maris Piper’ at a density of 180 tubers per plot in four rows (15 plants per row). Two extra rows were used as irrigation barriers between the plots. The soil was a sandy loam (67% sand, 27% silt, 13% clay, and 2.9% organic matter) Cambisol (World Reference Base). The compaction treatment was applied by successive passes of a tractor–drill–cultivator combination with high-pressure, row-crop tires on soil irrigated to field capacity before the formation of the ridges for tuber plantation. An ERT array of 24 electrodes (0.25-m electrode spacing) was used to collect resistivity transects on all plots of Block 3 by putting the electrodes in the furrows between the ridges (Figure 1b). The ERT data were collected on 12 June 2018 and 3 Aug. 2018. The ERT data were inverted with a background constrained approach using ResIPy (Blanchy, Saneiyan, Boyd, McLachlan, & Binley, 2020) that makes use of the R2 inverse code (Binley, 2015).

2.5.3 | Tillage and N treatments

The experiment aims at analyzing the impact of tillage and N fertilizer application on the growth of winter wheat and the associated soil moisture dynamics. It took place in a field, named “Pastures” (51°48′28.6“ N, 0°22′23.6″ W) managed by Rothamsted Research. The soil of the field is classified as a Luvisol (World Reference Base) with a clayey loamy texture. On 3 Oct. 2018, the experiment was sown with winter wheat. The experimental setup is composed of five blocks of 10 plots each (6 × 9 m). Two tillage treatments

TABLE 1 Summary of the experiments, devices used, and processing steps performed

Experiments	Devices	Processing steps
Impact of cover crops on soil moisture availability	EMI calibrated with ERT	Inversion of ERT transects Calibration of EMI data with inverted ERT (Lavoué et al., 2010) Temperature correction of calibrated ECa (Ma et al., 2011) Computing ΔECa from reference 22 July 2017 Inversion of ΔECa (Whalley et al., 2017)
Impact of compaction and irrigation on potato water uptake	ERT	Inversion of ERT transects Temperature correction of the inverted profiles (Ma et al., 2011) Computing ΔECa from reference 11 Mar. 2019
Impact of tillage and N fertilization on soil drying under winter wheat	EMI calibrated with ERT	Inversion of ERT transects Calibration of EMI data with inverted ERT (Lavoué et al., 2010) Temperature correction of calibrated ECa (Ma et al., 2011) Computing of ΔECa from reference 12 June 2018

Note. EMI, electromagnetic induction; ERT, electrical resistivity tomography; ECa, apparent electrical conductivity.

(direct drilling and conventional plowing) and five different N fertilizer rates (0, 80, 140, 180, and 220 kg N ha^{-1}) were applied by hand to each plot in two equal splits on 4 Mar. 2019 and 23 Apr. 2019. The tillage treatment was applied in bands across all the blocks, while the N fertilizers were randomly applied to each plot within a block (Figure 1c). The ERT arrays (24 pins, 0.25-m electrode spacing) were installed in four selected plots in the experiment to calibrate EMI measurements, following Lavoué et al. (2010). The ERT measurements were collected on 5 Feb. 2019, 5 Apr. 2019, 7 May 2019, 24 May 2019, 6 June 2019, 18 June 2019, 9 July 2019, 22 July 2019, and 5 Aug. 2019. The EMI measurements using the CMD Mini-Explorer were collected on 7 Dec. 2018, 5 Feb. 2019, 1 Mar. 2019, 4 Mar. 2019, 5 Mar. 2019, 7 Mar. 2019, 11 Mar. 2019, 13 Mar. 2019, 21 Mar. 2019, 5 Apr. 2019, 15 Apr. 2019, 30 Apr. 2019, 7 May 2019, 20 May 2019, 6 June 2019, 18 June 2019, 9 July 2019, 22 July 2019, and 5 Aug. 2019. The field had a large variability with ECa values ranging from 20 to 45 mS m^{-1}. Analysis of variance was used to detect significant differences ($p < .05$) between the treatments. Table 1 summarizes the different experiments, instrument used, and processing steps.

3 | RESULTS

3.1 | Cover crops

Figure 2 shows the evolution of the soil ECa (both apparent Figure 2a and inverted Figures 2b–d) for three selected cover crops and the bare soil treatment in 2016–2017. There is clear difference in ECa in November 2016 with higher values implying greater soil moisture content. The plots with tillage radish and white mustard exhibit significantly lower apparent conductivity than the bare soil or the vetch treatments. After the cover crops were destroyed (mowed) in December 2016, this difference is still visible, but starts to decrease. Finally, in March 2017, there is no difference between the bare soil and the cover crops treatments. Similar interpretation can be made using the profiles (Figures 2b–d) of inverted change in conductivity (changes are expressed from July 2017). There are differences between the bare soil and the cover crops in November 2016 that tend to decrease in December 2016 and vanish in March 2017.

Figure 3b shows the evolution of the ECa for the long-term cover crop experiment expressed as differences relative to 11 Mar. 2018. Given the amplitude of the signal in Figure 3b, for each survey date (t), we averaged all differences (ΔECa_t, which are still differences from 11 Mar. 2018) from all treatments to form the mean difference ($\overline{\Delta ECa_t}$). For each survey date, this mean was then subtracted from the difference for each treatment. This allows easier comparison between treatments (Figure 3c):

$$\Delta ECa_{i,t} - \overline{\Delta ECa_t} = \Delta ECa_{i,t} - \frac{1}{N}\sum \Delta ECa_{i,t} \quad (2)$$

where t is the index of the survey, i is the index of the treatment, N is the number of treatments, $\Delta ECa_{i,t}$ represents the differences relative to 11 Mar. 2018 for treatment i at survey date t, and $\overline{\Delta ECa_t}$ is the mean encompassing all treatments for the survey t.

Thus, Figure 3c removes the seasonal trend of Figure 3b and enhances the difference between treatments inside the same survey. The date 11 Mar. 2019 was chosen as a reference because it is the date with minimal effects of the treatments and most homogeneous ECa, all cover crops having been destroyed in the beginning of March. Figure 4 supports Figure 3 by showing subplots of differences in ECa for all varieties. Figure 3 and Figure 4 show data from VCP0.71 (the coil configuration that appears to be the most sensitive to the root zone). However, trends that are similar, albeit less strong than for other coil configurations,

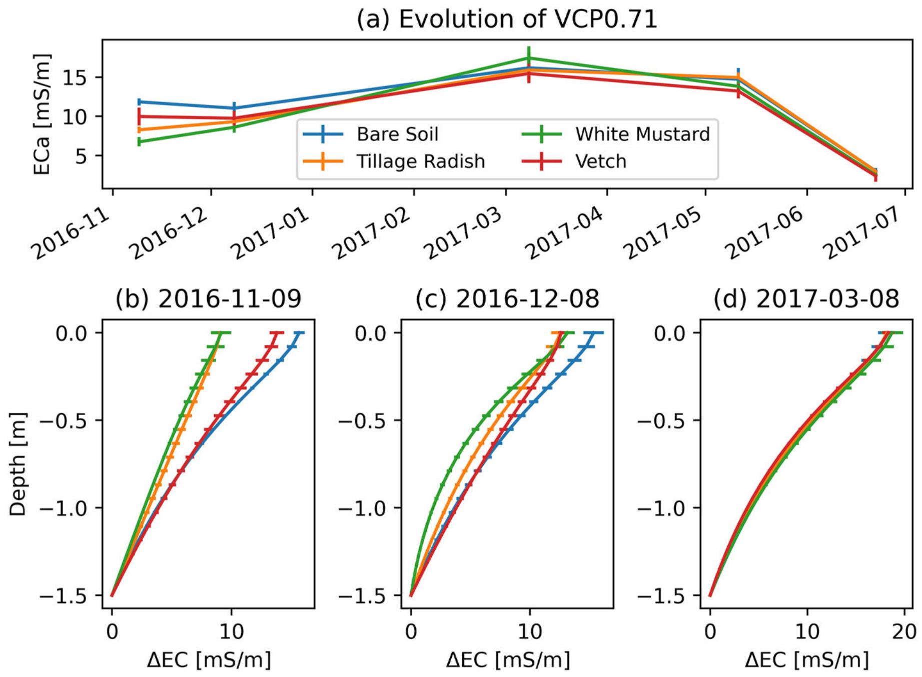

FIGURE 2 (a) The evolution of the apparent electrical conductivity (ECa) for four selected treatments: bare soil, tillage radish, white mustard, and vetch. (b–d) The inverted change in electrical conductivity (ΔEC) for three different dates. The inverted changes are computed as differences with respect to 22 July 2017 (dry reference)

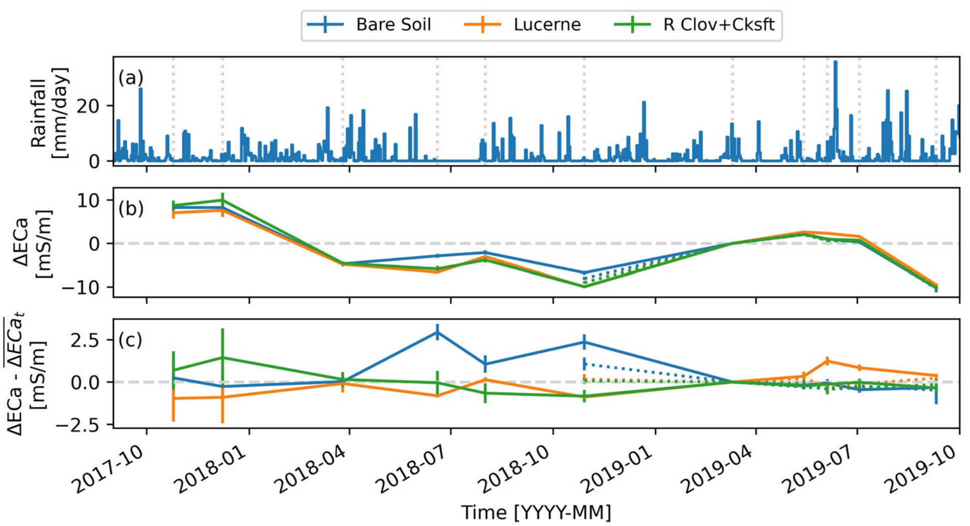

FIGURE 3 Evolution of the difference in apparent electrical conductivity of VCP0.71 for bare soil, lucerne, and red clover + cocksfoot (R Clov + Cksft) treatments in place for 1 yr (dotted lines) and 2 yr (solid lines). (a) The daily rainfall. (b) The difference in apparent electrical conductivity (ΔECa) compared with the reference date 11 Mar. 2019. To make the difference between treatments more visible, the average difference for all treatments is computed for each survey ($\overline{\Delta ECa_t}$) and is subtracted from Panel b leading to Panel c. Error bars represent the standard error of the mean

can also be observed. Both short-term (sown in September 2018) and long-term (sown in September 2017) cover crops show a significant difference compared with the bare soil treatments (19 June 2018, 1 Aug. 2018, and 29 Oct. 2018 in Figure 4). This can be seen over summer 2018 (Figure 3a). The long-term cover crops also tend to show a larger difference in ECa than the short-term cover crops (29 Oct. 2018 in Figure 4). For the long-term chicory and lucerne, two deep-rooting cover crops, this difference stays significant even in June and July 2019, but not for their short-term equivalent. Note that the magnitude of this difference is relatively small (~2 mS m^{-1}) and thus does not represent a large difference in soil moisture (only a few percent). The other shallower rooting cover crops, such as the red clover

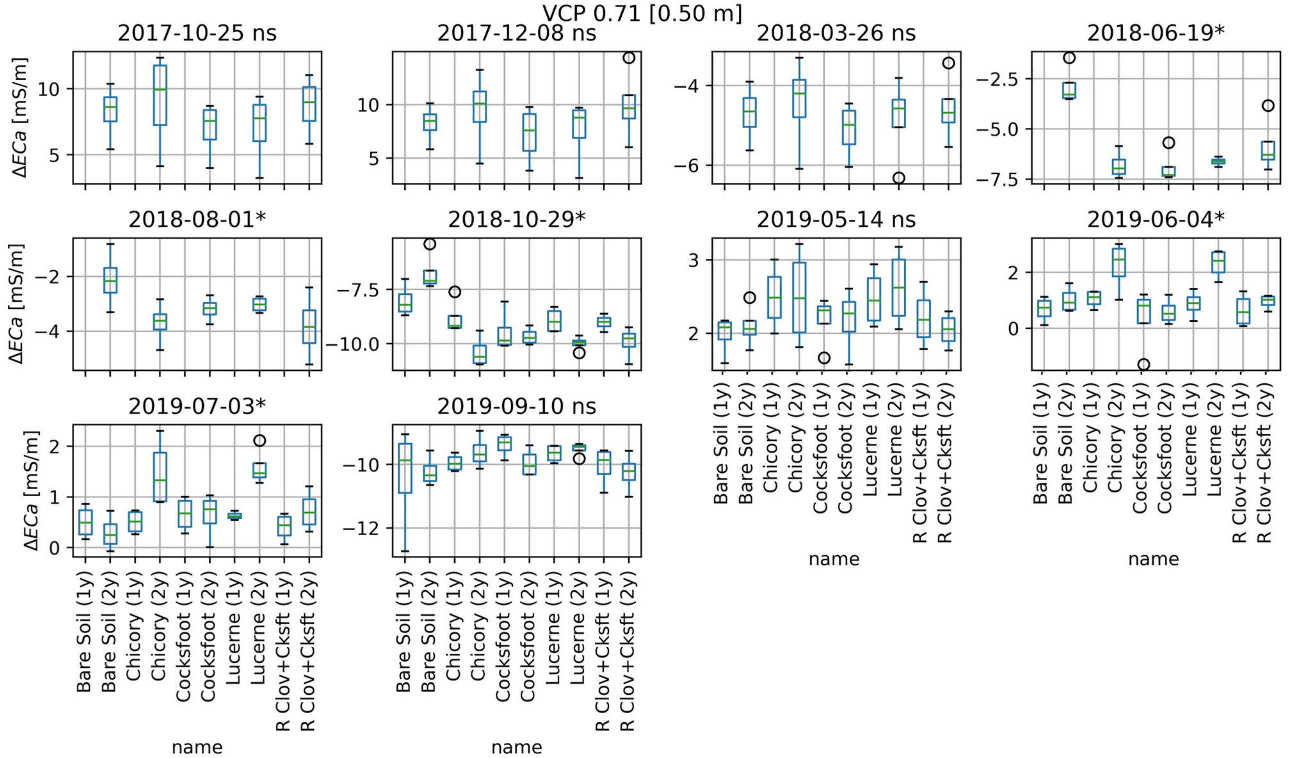

FIGURE 4 Subplots of boxplots showing the differences in apparent electrical conductivity (ΔECa) compared with the reference date 11 Mar. 2019. Long-term cover crops are indicated by "2y," and short-term cover crops are indicated by "1y." An asterisk above the graph shows that there are significant differences ($p < .05$) from an ANOVA test between the treatments. No-significant results are denoted by "ns." Each subplot has its own vertical scale. R Clov + Cksft, red clover + cocksfoot

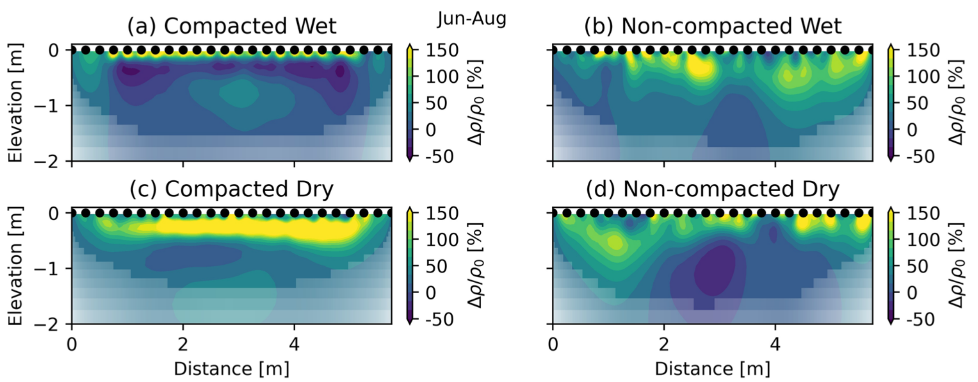

FIGURE 5 Relative change in inverted resistivity ($\Delta\rho/\rho_0$) section between 12 June and 3 Aug. 2018 showing the different treatments: (a) compacted wet, (b) noncompacted wet, (c) compacted dry, and (d) noncompacted dry. Note that the resistivity is the inverse of the conductivity. The semitransparent white overlay shows the sensitivity of the survey

and cocksfoot, do not show any effect in June or July 2019 for both short- and long-term variants.

3.2 | Compaction and irrigation

After inverting each survey, the difference in resistivity from June 2018 to August 2018 ($\Delta\rho$) is computed and divided by the resistivity of the first survey taken on 12 June 2018 (ρ_0) to obtain a relative difference. Figure 5 shows the relative difference in inverted resistivity ($\Delta\rho/\rho_0$ expressed as a percentage) sections with the yellow area associated with an increase in resistivity (drying) and the blue area associated with a decrease in resistivity (wetting). All sections show a larger positive change, probably associated with soil drying close to the surface, extending no deeper than 0.7 m. The compacted wet treatment shows the shallowest drying by the crop, whereas the noncompacted treatments exhibits deeper drying. Figures 5a and c

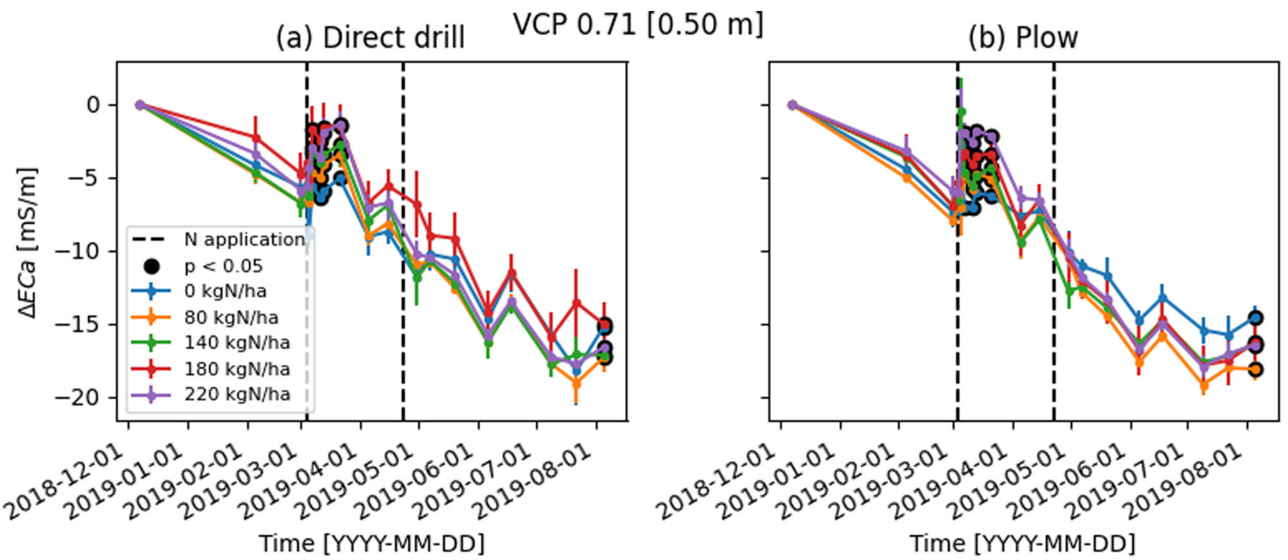

FIGURE 6 Evolution of the differences in apparent conductivity (ΔECa) for VCP0.71 according to (a) direct drill and (b) plow treatment. The vertical dotted lines indicate when fertilizer was applied. Black dots show where the difference between the fertilizer treatments is significant ($p < .05$ by ANOVA). Error bars represent the standard error of the mean

also clearly show the depth of drying is limited, probably by the compaction, compared with noncompacted treatments (Figures 5b and d). No treatments showed any major differences in resistivity deeper than approximately 1.5-m depth.

3.3 | Tillage and N treatments

In October 2018, there was a significant ($p < .05$ by ANOVA) difference in absolute ECa between the plow and the direct drill treatments prior to any drying by the crops or application of N. The direct drill plots show a higher ECa than the plowed plots (data not shown). To remove the effect of this initial difference, the change in ECa is computed by subtracting the values measured on 7 Dec. 2018 (reference date). Figure 6 shows that N levels only had a significant effect on ECa for a few days after the first fertilizer application, where the ECa changes were correlated to the N rates (Figure 7). The N fertilizer increases the ECa proportionally to the application rates, but because differences in ECa are used and there is a general ECa decrease throughout the season, the inverse relationship is observed. Despite having no significant effect later on in the season, it can still be observed that the plots that did not receive additional N fertilizer (0 kg N ha^{-1}) are distinct from the other plots from May onwards in the plow treatment. This cannot be observed in the direct drill treatment. Figure 8 shows the main effect of tillage treatment. Both plow and direct drill treatments show a decrease through the season probably related to soil drying. We observe that the difference between direct drill and plow treatments increases after the second application of fertilizer for most

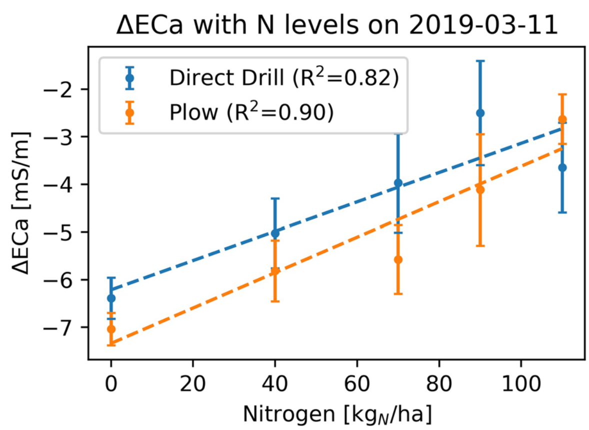

FIGURE 7 Differences in apparent electrical conductivity (ΔECa) as a function of the amount of nitrogen after the first application (nitrogen applied on 2019-03-04). Note that differences are taken with respect to the reference date 2018-12-07 and not just before the nitrogen application. This is why large amount of fertilizer actually shows a smaller decrease in ECa as they compensate more the global ECa decreases from the reference date

EMI coil configurations, especially those that were more sensitive to deeper layers. These differences are not significant anymore after the 1 July. The N fertilizer rate had a significant impact on the yield (Figure 9). Nitrogen fertilizer was more effective at increasing yield in the plow treatment compared with the direct drill treatment, particularly at the higher rates of N. This effect is also seen in the development of the leaf area index (LAI, Figure 10). Between mid-May and mid-June, the LAI in the direct drill treatments continues to increase. In the plow treatments, the

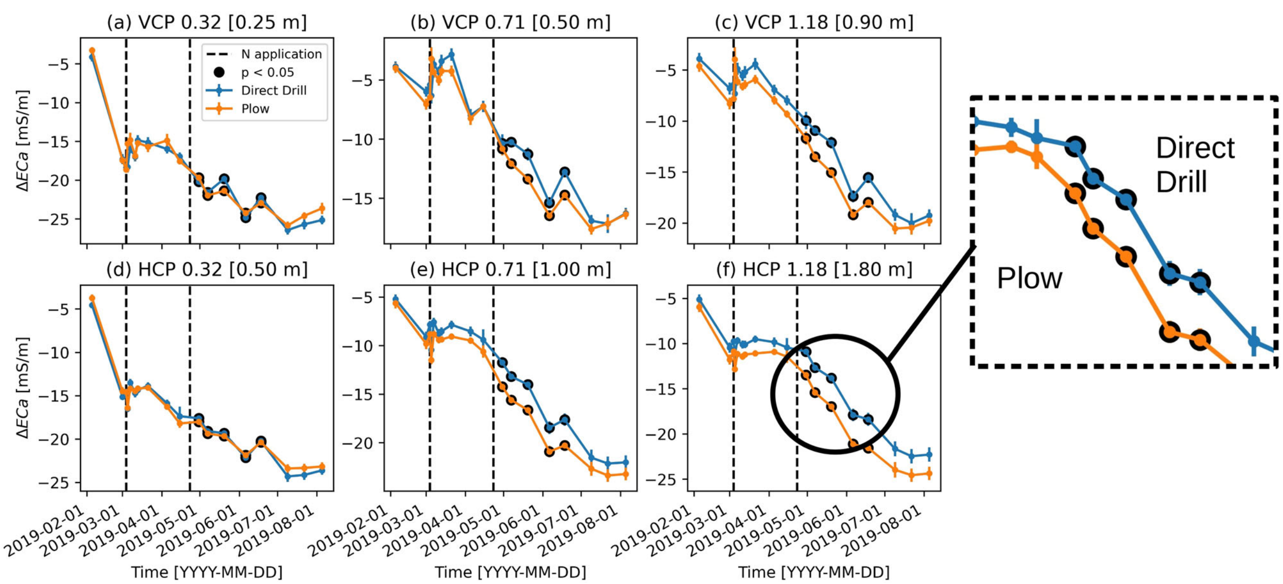

FIGURE 8 Evolution of the differences in apparent electrical conductivity (ΔECa) with respect to the reference date 7 Dec. 2018 for the six coil configurations of the CMD Mini-Explorer (a–f). All plots have been averaged between direct drill and plow treatment. Error bars represent standard error of the mean. Black dots show where the difference between direct drill and plow treatment is significant ($p < .05$ by ANOVA)

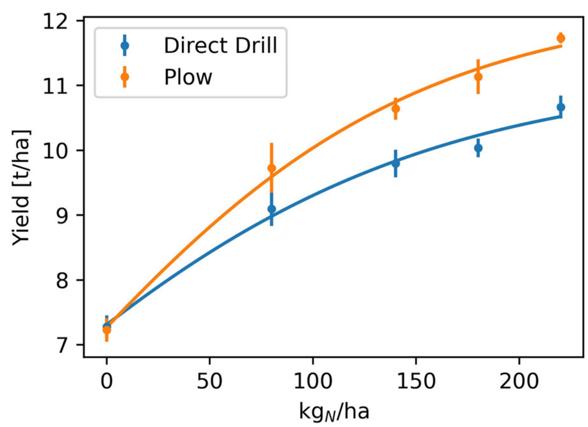

FIGURE 9 Yield response to the amount of N fertilizer for the direct drill and plow treatments. Error bars represent the standard error of the mean. A sigmoid $\{a/[b + \exp(-cx + d)]\}$ has been fitted to both curves

LAI reaches its maximum mid-May and does not substantially increase from mid-May to mid-June.

4 | DISCUSSION

4.1 | Capabilities

A single geophysical survey can be useful to map soil textural variation across the field and, in some cases, can be linked to soil moisture distribution (Calamita et al., 2012). However, there is little information on how it might affect crop productivity. Time-lapse geophysical surveys, in contrast, enable to some extent the removal the static effects of soil properties on the geophysical measurements. Changes in EC (or ECa), once temperature corrected, can then more easily be linked to changing states such as soil moisture or pore water ionic concentration. In the case studies presented here, which took place in nonsaline environments, we can reasonably link the changes in ECa to the changes in soil moisture due to crop water uptake (evapotranspiration). We also observed that during short periods immediately after the application on mineral N, there was a sudden increase in EC, probably due to an increase in pore water EC (Figure 6).

In the first case study, cover crops were found to have a significant effect compared with the bare soil in the first and second experiments. In November 2016, the tillage radish and white mustard had a larger effect than the vetch. However, after mowing, no more effect of the cover crops on the soil dynamics was observed. In the second experiment, both short-term and long-term cover crops show significant effect compared with the bare soil. Cover crops in place for 2 yr tend to have a larger effect compared with cover crops grown for one season (Figure 4). After being cut down, most cover crop treatments do not show any difference compared with bare soil. Only the long-term chicory and lucerne, two deep-rooting cover crops, show a significant effect in June and July 2019 (Figure 3 and 4). These ECa differences in the long-term chicory and lucerne treatments on 4 June 2019 (Figure 4) could be caused by an improved soil structure allowing better rainfall infiltration and possibly larger moisture

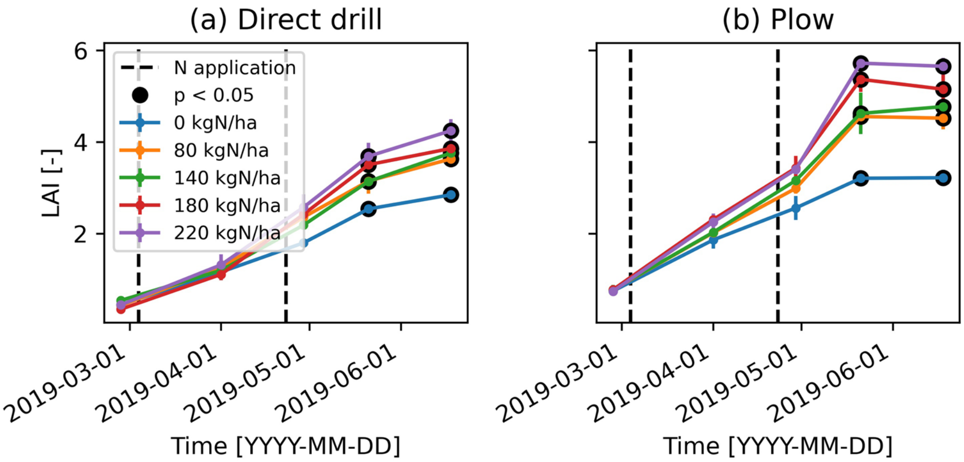

FIGURE 10 Evolution of the leaf area index (LAI) between (a) direct drill and (b) plow treatments split by amount of N fertilizers applied. Black dots show where the difference between the fertilizer treatments is significant ($p < .05$ by ANOVA). Error bars represent the standard error of the mean

storage. Ren, Vanden Nest, Ruysschaert, D'Hose, and Cornelis (2019) found that white mustard has a positive effect on the soil structure, promoting deeper root penetration of maize crop. However, the magnitude of the change (a few mS m^{-1}), once converted to soil moisture, only represents a few percent, hence not constituting a substantial difference in soil drying compared with other treatments. Analysis of changes in ECa enhances the differences between cover crops, which would be less obvious with absolute ECa values, as part of the signal would be affected by various soil textures across the field.

Potatoes are particularly sensitive to drought stress. Although Tang, Farooque, Bos, and Abbas (2019) attempted to directly relate ECa to soil moisture and potato tuber yield, the second case study presented here focused on the impact of traffic-induced compaction and irrigation treatment on the soil moisture. Time-lapse ERT between potato ridges revealed the limited depth of water uptake in compacted soil compared with noncompacted treatments. Plants in the noncompacted treatments can probably access water at a greater depth more easily (and thus dry the soil) in comparison with the compacted treatments. In wet treatments, crops rely mainly on the water stored in the top 30–40 cm of soil. One major disadvantage of placing the electrodes in the furrows is that no information can be collected on what is happening inside the ridges. However, this setup enables us to better measure the effect of compaction, as all ridges are compaction free. Such information is potentially useful for agronomists to adapt agricultural practices, such as irrigation schedules tailored to canopy and root development. Minimally invasive ERT or EMI survey could reveal depth of drying of the crop and help more accurately estimate the amount of water needed for irrigation, leading to more cost-effective management of the water resource.

Time-lapse EMI in the third case study revealed that direct drill and plow treatments influence the soil moisture dynamics and the N uptake by the crop. From Figure 1c, it can be observed that direct drill resulted in patchier plots, mainly due to the lower survival rate of the plants in the direct drill plots over winter. During the growing season, direct drill plots showed a somewhat smaller rate of decrease in ECa (Figure 8). It is probably the case that the direct drilled plots remained wetter due to a combination of lower evapotranspiration losses from a lower leaf area (Figure 10) and a more restricted root system. This is consistent with Sławiński, Cymerman, Witkowska-Walczak, and Lamorski (2012), who found greater soil moisture in reduced tillage compared with conventional tillage, for 3 yr of winter wheat monoculture on two different soils. The potential decrease in porosity in the plow treatment during the season could have increased the ECa. However, given that a general decrease in ECa is observed, this effect is probably minor compared with the change in soil moisture. Nevertheless, it could lead to an underestimation of the soil drying in the plow treatment based on ECa changes. The addition of N fertilizer caused a significant increase in ECa over a short period (Figure 6). The changes in ECa correlates well with the amount of N supplied (Figure 7). This is in accordance with the results of Eigenberg, Doran, Nienaber, Ferguson, and Woodbury (2002), who successfully use EMI for monitoring different N uptakes. However, this effect was only observed after the first application of fertilizer (4 Mar. 2019) and not the second (23 Apr. 2019). This could be because of a more rapid N uptake due to larger plants at the second application. In contrast, the LAI started to increase proportionally to the N level after the second application (Figure 10). This increase in LAI potentially led to larger soil drying and might be the cause of the significant differences observed between the tillage treatments (Figure 8). Yield response to the different rates was also larger for the plow than for the direct drill treatment (Figure 9). One possible explanation is that the larger root impedance in direct drill treatments led to a less effective use of N fertilizer (Ge et al., 2019). However, without additional N, both plow and direct drill treatments had similar yield. Overall, time-lapse EMI enables us to obtain information on the soil moisture and N dynamics taking place in different tillage treatments.

4.2 | Limitations and recommendations

The cases we describe demonstrate that the minimal invasive operation of EMI and its high throughput are significant advantages of this method for agricultural applications. In some cases, EMI surveys can even be conducted while the crop is still in place (e.g., placing the instrument between the rows of wheat or the ridges of potatoes without damaging the crop). For its part, the greater resolution of ERT allows better recovery of depth-specific properties at the expense of a more complex setup. The two methods have the advantage of sampling a relatively large volume of soil, producing more representative measurements than conventional soil sampling or soil moisture sensing. Although both methods can be used for one-time survey, time-lapse studies clearly have great potential for agricultural studies, as they enable the observation of the variation of states that can be related to plant development and plant productivity.

The EMI instruments are sensitive to measurement drift, and for our case studies, we let the instrument warm up to outdoor temperature for at least 30 min before starting the data collection (following Shanahan et al., 2015). Additionally, the setup of a drift station, a place where measurements are collected at regular time interval, is recommended. More complex drift correction can also be applied (Delefortrie, De Smedt, Saey, Van De Vijver, & Van Meirvenne, 2014; Robinson, Lebron, Lesch, & Shouse, 2004). This procedure is essential for time-lapse surveys, as it is likely that the drift of one survey will be different from another survey, inducing bias in the analysis. Temperature corrections are also essential in time-lapse surveys as mentioned in Section 2.4, as the soil temperature is an important factor contributing to the soil EC.

Calibration of EMI, possibly by using an ERT array (Lavoué et al., 2010; von Hebel et al., 2019), helps to transform qualitative EMI data to more quantitative values. However, it requires that ERT and EMI data span a sufficient range of EC values (in time or in space) in order to build a strong relationship, which can be a limitation in some situation. In our case, robust calibration equations were obtained for the wheat experiment using four time-lapse ERT arrays across the field and using a single time-lapse ERT array for the cover crop experiments.

Multi-coil EMI instruments now enable the inversion of ECa data to depth-specific EC. However, this inversion remains challenging given the usual small number of coil configurations. Indeed, although ERT datasets usually consist of hundreds if not thousands of quadrupoles providing overlapping information on the same soil volume, EMI datasets usually rely on a few coil configurations. Smoothed Gauss–Newton solution (Whalley et al., 2017), Markov chain Monte Carlo methods (Shanahan et al., 2015), or the shuffle complex algorithm (von Hebel et al., 2014) are a few of the available methods for one-dimensional inversion of EMI data.

Although the above precautions are not needed with ERT instruments, the electrode setup and acquisition are more important. Electrodes, after initial installation, can be left in place while the crop is growing, allowing time-lapse measurements to be taken at the same exact position. This enables ERT surveys to be inverted using difference inversion (LaBrecque & Yang, 2001). The drawback of that is that soils with high clay content will tend to swell and shrink, eventually leading to desiccation cracks around the electrodes (point of stress concentration) undermining the galvanic contact needed for ERT acquisition. Such effects have led some authors to explore the use of ERT to detect cracks in soils (Hassan & Toll, 2013; Samouëlian, Cousin, Richard, Tabbagh, & Bruand, 2003; Samouëlian et al., 2004). Using a mobile ERT array that is set up for each survey can be an alternative but requires more precautions to not damage the growing crop during installation. Given that the electrodes are unlikely to be at the same exact positions as previous surveys, a difference inversion cannot be used, but inversion with constraint to a reference dataset can be adopted (as is the case here). Once inverted, ERT sections also need to be temperature corrected.

Relating soil EC to soil properties or state is ultimately challenging. This is because EC is influenced by many factors (texture, density, pore water EC, soil moisture, and temperature). These factors need to be controlled or accounted for to develop an EC value that relates the property of interest. Pedophysical relationships linking geophysical properties to soil properties are often site specific and can be nonlinear (Calamita et al., 2012; Laloy et al., 2011). Although this manuscript does not attempt to convert change in EC to soil moisture content, we believe that the time-lapse approach and data processing carried out allow for the previous interpretations to be made. However, if changes in other soil properties, such as the decrease in porosity from tillage during the season, were to be observed with geophysical instruments, independent measurements of the soil moisture variation would be needed in order to better isolate the contribution of the change in porosity to the ECa variation.

The three case studies presented in this work were applied to relatively small plots from research sites. However, the geophysical methods proposed, particularly EMI, has the potential to map much larger areas (Brogi et al., 2019). Electrical resistivity tomography systems, mounted on towed system (e.g., Veris Quad EC 1000), also allow mapping of large area. However, because ERT requires galvanic contact with the soil, it might be challenging to use a towed system without damaging a growing crop.

Finally, other geophysical methods such as acoustic–seismic (Lu, 2014), ground-penetrating radar (Akinsunmade, Tomecka-Suchoń, & Pysz, 2019; Algeo, Slater, Binley, Van Dam, & Watts, 2018; Klenk, Jaumann, & Roth, 2015; Klotzsche et al., 2019), or even nuclear magnetic resonance (Paetzold, Matzkanin, & Santos, 1985) are emerging methods that have potential for agricultural applications.

5 | CONCLUSION

Time-lapse EMI and ERT surveys detect changes in EC that can more easily be related to variable states, such as soil moisture, compared with conventional static (one-time) surveys. The collection of case studies reported here illustrates the effectiveness of time-lapse geophysics for a range of applications. The time-lapse approach helps to monitor cover crop effect on soil drying and image the reduced depth of water uptake in compacted soil for potatoes. Under winter wheat, a plow-based treatment showed larger decrease in ECa associated with larger soil drying compared with a direct drill treatment, which might explain the yield gap observed. Significant correlation between the different level of N and the ECa changes was also found, but only for a short period of time. In contrast, yield and LAI showed a stronger response to N levels in plow than in direct drill treatment. Although interpretation of geophysical data should always be done carefully, we believe that the use of the time-lapse approach for the EMI and ERT dataset have great potential to monitor the effects of a range of agricultural practices.

CONFLICT OF INTEREST

The authors declare no conflict of interest.

ACKNOWLEDGMENTS

G.B. is supported by a Lancaster University–Rothamsted Research–Center for Ecology & Hydrology Graduate School for Environment PhD studentship. M.J.H and W.R.W. at Rothamsted Research are supported by the Designing Future Wheat Program by the UK Biotechnology and Biological Sciences Research Council (BB/P016855/1). One field site for the long-term cover crop experiment was fully funded by the British Beet Research Organisation (BBRO), and the second field was funded by a joint University of Nottingham (50%)–BBRO (50%) studentship. The work on compaction and irrigation was funded under AHDB-Lancaster Contracts 110002102 and 110002104 (Applications of precision farming technologies to enhance rotations). The pasture experiment was funded by Biotechnology and Biological Sciences Research Council Institute Strategic Programme grants Delivering Sustainable Systems (BB/J004286/1) and Soil to Nutrition (S2N, BBS/E/C/00I0330). We are grateful for the comments received from two anonymous reviewers—their input strengthened the manuscript.

ORCID

Guillaume Blanchy https://orcid.org/0000-0001-6341-5826
Chris. W. Watts https://orcid.org/0000-0002-7223-1444
Malcolm J. Hawkesford https://orcid.org/0000-0001-8759-3969
W. Richard Whalley https://orcid.org/0000-0003-0755-2943
Andrew Binley https://orcid.org/0000-0002-0938-9070

REFERENCES

Akinsunmade, A., Tomecka-Suchoń, S., & Pysz, P. (2019). Correlation between agrotechnical properties of selected soil types and corresponding GPR response. *Acta Geophysica*, *67*, 1913–1919. https://doi.org/10.1007/s11600-019-00349-4

Algeo, J., Slater, L., Binley, A., Van Dam, R. L., & Watts, C. (2018). A comparison of ground-penetrating radar early-time signal approaches for mapping changes in shallow soil water content. *Vadose Zone J*, *17*(1). https://doi.org/10.2136/vzj2018.01.0001

Allred, B.J., Daniels J.J., & Ehsani M.R. (Eds.). (2008). *Handbook of agricultural geophysics*. Boca Raton, FL: CRC Press.

Amundson, R., Berhe, A. A., Hopmans, J. W., Olson, C., Sztein, A. E., & Sparks, D. L. (2015). Soil and human security in the 21st century. *Science*, *348*, 1261071–1261071. https://doi.org/10.1126/science.1261071

Archie, G. E. (1942). The electrical resistivity log as an aid in determining some reservoir characteristics. *Transactions of the AIME*, *146*, 54–62. https://doi.org/10.2118/942054-G

Batey, T. (2009). Soil compaction and soil management: A review. *Soil Use Management*, *25*, 335–345. https://doi.org/10.1111/j.1475-2743.2009.00236.x

Binley, A. (2015). Tools and techniques: Electrical methods. In G. Schubert (Ed.), *Treatise on geophysics* (2nd ed., pp. 233–259). Oxford, UK: Elsevier.

Binley, A., Hubbard, S. S., Huisman, J. A., Revil, A., Robinson, D. A., Singha, K., & Slater, L. D. (2015). The emergence of hydrogeophysics for improved understanding of subsurface processes over multiple scales: The emergence of hydrogeophysics. *Water Resources Research*, *51*, 3837–3866. https://doi.org/10.1002/2015WR017016

Blanchy, G., Saneiyan, S., Boyd, J., McLachlan, P., & Binley, A. (2020). ResIPy, an intuitive open source software for complex geoelectrical inversion/modeling. *Computers & Geosciences*, *137*. https://doi.org/10.1016/j.cageo.2020.104423

Blanchy, G., Watts, C. W., Ashton, R. W., Webster, C. P., Hawkesford, M. J., Whalley, W. R., & Binley, A. (2020). Accounting for heterogeneity in the θ–σ relationship: Application to wheat phenotyping using EMI. *Vadose Zone Journal*, *19*(1). https://doi.org/10.1002/vzj2.20037

Boaga, J. (2017). The use of FDEM in hydrogeophysics: A review. *Journal of Applied Geophysics*, *139*, 36–46. https://doi.org/10.1016/j.jappgeo.2017.02.011

Brogi, C., Huisman, J. A., Pätzold, S., von Hebel, C., Weihermüller, L., Kaufmann, M. S., … Vereecken, H. (2019). Large-scale soil mapping using multi-configuration EMI and supervised image classification. *Geoderma*, *335*, 133–148. https://doi.org/10.1016/j.geoderma.2018.08.001

Calamita, G., Brocca, L., Perrone, A., Piscitelli, S., Lapenna, V., Melone, F., & Moramarco, T. (2012). Electrical resistivity and TDR methods for soil moisture estimation in central Italy test-sites. *Journal of Hydrology*, *454–455*, 101–112. https://doi.org/10.1016/j.jhydrol.2012.06.001

Calamita, G., Perrone, A., Brocca, L., Onorati, B., & Manfreda, S. (2015). Field test of a multi-frequency electromagnetic induction sensor for soil moisture monitoring in southern Italy test sites. *Journal of Hydrology*, *529*, 316–329. https://doi.org/10.1016/j.jhydrol.2015.07.023

Callegary, J. B., Ferré, T. P. A., & Groom, R. W. (2007). Vertical spatial sensitivity and exploration depth of low-induction-number electromagnetic-induction instruments. *Vadose Zone Journal*, *6*, 158–167. https://doi.org/10.2136/vzj2006.0120

Cimpoiaşu, M. O., Kuras, O., Pridmore, T., & Mooney, S. J. (2020). Potential of geoelectrical methods to monitor root zone processes and structure: A review. *Geoderma*, *365*. https://doi.org/10.1016/j.geoderma.2020.114232

Corwin, D. L., & Lesch, S. M. (2005). Apparent soil electrical conductivity measurements in agriculture. *Computers and Electronics in Agriculture*, *46*, 11–43. https://doi.org/10.1016/j.compag.2004.10.005

Delefortrie, S., De Smedt, P., Saey, T., Van De Vijver, E., & Van Meirvenne, M. (2014). An efficient calibration procedure for correction of drift in EMI survey data. *Journal of Applied Geophysics*, *110*, 115–125. https://doi.org/10.1016/j.jappgeo.2014.09.004

Doolittle, J. A., & Brevik, E. C. (2014). The use of electromagnetic induction techniques in soils studies. *Geoderma*, *223–225*, 33–45. https://doi.org/10.1016/j.geoderma.2014.01.027

Eigenberg, R. A., Doran, J. W., Nienaber, J. A., Ferguson, R. B., & Woodbury, B. L. (2002). Electrical conductivity monitoring of soil condition and available N with animal manure and a cover crop. *Agriculture, Ecosystems & Environment*, *88*, 183–193. https://doi.org/10.1016/S0167-8809(01)00256-0

Fageria, N. K., Baligar, V. C., & Bailey, B. A. (2005). Role of cover crops in improving soil and row crop productivity. *Communications in Soil Science and Plant Analysis*, *36*, 2733–2757. https://doi.org/10.1080/00103620500303939

Ge, Y., Hawkesford, M. J., Rosolem, C. A., Mooney, S. J., Ashton, R. W., Evans, J., & Whalley, W. R. (2019). Multiple abiotic stress, nitrate availability and the growth of wheat. *Soil and Tillage Research*, *191*, 171–184. https://doi.org/10.1016/j.still.2019.04.005

Hamza, M. A., & Anderson, W. K. (2005). Soil compaction in cropping systems: A review of the nature, causes and possible solutions. *Soil and Tillage Research*, *82*, 121–145. https://doi.org/10.1016/j.still.2004.08.009

Hassan, A., & Toll, D. G. (2013). Electrical resistivity tomography for characterizing cracking of soils. In C. Meehan, D. Pradel, M. A. Pando, & J. F. Labuz (Eds.), *Geo-Congress 2013: Stability and performance of slopes and embankments III* (pp. 818–827). Reston, VA: American Society of Civil Engineers. https://doi.org/10.1061/9780784412787.083

Hayashi, M. (2004). Temperature-electrical conductivity relation of water for environmental monitoring and geophysical data inversion. *Environmental Monitoring and Assessment*, *96*, 119–128. https://doi.org/10.1023/B:EMAS.0000031719.83065.68

Hedley, C. B., Yule, I. J., Eastwood, C. R., Shepherd, T. G., & Arnold, G. (2004). Rapid identification of soil textural and management zones using electromagnetic induction sensing of soils. *Australian Journal of Soil Research*, *42*, 389–400. https://doi.org/10.1071/SR03149

Hobbs, P. R., Sayre, K., & Gupta, R. (2008). The role of conservation agriculture in sustainable agriculture. *Philosophical Transactions of the Royal Society B: Biological Sciences*, *363*, 543–555. https://doi.org/10.1098/rstb.2007.2169

Jayawickreme, D. H., Jobbágy, E. G., & Jackson, R. B. (2014). Geophysical subsurface imaging for ecological applications. *New Phytologist*, *201*, 1170–1175. https://doi.org/10.1111/nph.12619

Keller, T., Colombi, T., Ruiz, S., Manalili, M. P., Rek, J., Stadelmann, V., … Or, D. (2017). Long-term soil structure observatory for monitoring post-compaction evolution of soil structure. *Vadose Zone Journal*, *16*(4). https://doi.org/10.2136/vzj2016.11.0118

Keller, T., Lamand, M., Peth, S., Berli, M., Delenne, J. Y., Baumgarten, W., … Or, D. (2013). An interdisciplinary approach towards improved understanding of soil deformation during compaction. *Soil and Tillage Research*, *128*, 61–80. https://doi.org/10.1016/j.still.2012.10.004

Klenk, P., Jaumann, S., & Roth, K. (2015). Quantitative high-resolution observations of soil water dynamics in a complicated architecture using time-lapse ground-penetrating radar. *Hydrology and Earth System Sciences*, *19*, 1125–1139. https://doi.org/10.5194/hess-19-1125-2015

Klotzsche, A., Lärm, L., Vanderborght, J., Cai, G., Morandage, S., Zörner, M., … Kruk, J. (2019). Monitoring soil water content using time-lapse horizontal borehole GPR data at the field-plot scale. *Vadose Zone Journal*, *18*(1). https://doi.org/10.2136/vzj2019.05.0044

LaBrecque, D. J., & Yang, X. (2001). Difference inversion of ERT data: A fast inversion method for 3-D in situ monitoring. *Journal of Environmental & Engineering Geophysics*, *6*, 83–89. https://doi.org/10.4133/JEEG6.2.83

Laloy, E., Javaux, M., Vanclooster, M., Roisin, C., & Bielders, C. L. (2011). Electrical resistivity in a loamy soil: Identification of the appropriate pedo-electrical model. *Vadose Zone Journal*, *10*, 1023–1033. https://doi.org/10.2136/vzj2010.0095

Lavoué, F., Van Der Kruk, J., Rings, J., André, F., Moghadas, D., Huisman, J. A., … Vereecken, H. (2010). Electromagnetic induction calibration using apparent electrical conductivity modelling based on electrical resistivity tomography. *Near Surface Geophysics*, *8*, 553–561. https://doi.org/10.3997/1873-0604.2010037

Lu, Z. (2014). Feasibility of using a seismic surface wave method to study seasonal and weather effects on shallow surface soils. *Journal of Environmental & Engineering Geophysics*, *19*, 71–85. https://doi.org/10.2113/JEEG19.2.71

Ma, R., McBratney, A., Whelan, B., Minasny, B., & Short, M. (2011). Comparing temperature correction models for soil electrical conductivity measurement. *Precision Agriculture*, *12*, 55–66. https://doi.org/10.1007/s11119-009-9156-7

McLachlan, Paul, Blanchy, Guillaume, & Binley, Andrew (2020). EMagPy: Open-source standalone software for processing, forward modeling and inversion of electromagnetic induction data. *Computers & Geosciences*. https://doi.org/10.1016/j.cageo.2020.104561 (in press).

Paetzold, R. F., Matzkanin, G. A., & Santos, A. D. L. (1985). Surface soil water content measurement using pulsed nuclear magnetic resonance techniques. *Soil Science Society of America Journal*, *49*, 537–540. https://doi.org/10.2136/sssaj1985.03615995004900030001x

Ren, L., Vanden Nest, T., Ruysschaert, G., D'Hose, T., & Cornelis, W. M. (2019). Short-term effects of cover crops and tillage methods on soil physical properties and maize growth in a sandy loam soil. *Soil and Tillage Research*, *192*, 76–86. https://doi.org/10.1016/j.still.2019.04.026

Rhoades, J. D., Raats, P. A. C., & Prather, R. J. (1976). Effects of liquid-phase electrical conductivity, water content, and surface conductivity on bulk soil electrical conductivity. *Soil Science Society of America Journal*, *40*, 651–655. https://doi.org/10.2136/sssaj1976.03615995004000050017x

Robinson, D. A., Lebron, I., Lesch, S. M., & Shouse, P. (2004). Minimizing drift in electrical conductivity measurements in high temperature environments using the EM-38. *Soil Science Society of America Journal*, *68*, 339–345. https://doi.org/10.2136/sssaj2004.3390

Romero-Ruiz, A., Linde, N., Keller, T., & Or, D. (2018). A review of geophysical methods for soil structure characterization: Geophysics and soil structure. *Reviews of Geophysics*, *56*, 672–697. https://doi.org/10.1029/2018RG000611

Samouëlian, A., Cousin, I., Richard, G., Tabbagh, A., & Bruand, A. (2003). Electrical resistivity imaging for detecting soil cracking at the centimetric scale. *Soil Science Society of America Journal*, *67*, 1319–1326. https://doi.org/10.2136/sssaj2003.1319

Samouëlian, A., Cousin, I., Tabbagh, A., Bruand, A., & Richard, G. (2005). Electrical resistivity survey in soil science: A review. *Soil and Tillage Research*, *83*, 173–193. https://doi.org/10.1016/j.still.2004.10.004

Samouëlian, A., Richard, G., Cousin, I., Guerin, R., Bruand, A., & Tabbagh, A. (2004). Three-dimensional crack monitoring by electrical resistivity measurement. *European Journal of Soil Science*, *55*, 751–762. https://doi.org/10.1111/j.1365-2389.2004.00632.x

Schlumberger, C. (1920). *Etude sur la prospection electrique du sous-sol*. Gauthier-Villars.

Shanahan, P. W., Binley, A., Whalley, W. R., & Watts, C. W. (2015). The use of electromagnetic induction to monitor changes in soil moisture profiles beneath different wheat genotypes. *Soil Science Society of America Journal*, *79*, 459–466. https://doi.org/10.2136/sssaj2014.09.0360

Sławiński, C., Cymerman, J., Witkowska-Walczak, B., & Lamorski, K. (2012). Impact of diverse tillage on soil moisture dynamics. *International Agrophysics*, *26*, 301–309. https://doi.org/10.2478/v10247-012-0043-5

Tan, X., Mester, A., von Hebel, C., Zimmermann, E., Vereecken, H., van Waasen, S., … van der Kruk, J. (2019). Simultaneous calibration and inversion algorithm for multiconfiguration electromagnetic induction data acquired at multiple elevations. *Geophysics*, *84*, EN1–EN14. https://doi.org/10.1190/geo2018-0264.1

Tang, S., Farooque, A. A., Bos, M., & Abbas, F. (2019). Modelling DUALEM-2 measured soil conductivity as a function of measuring depth to correlate with soil moisture content and potato tuber yield. *Precision Agriculture*, *21*, 484–502. https://doi.org/10.1007/s11119-019-09678-2

Viscarra Rossel, R. A., Adamchuk, V. I., Sudduth, K. A., McKenzie, N. J., & Lobsey, C. (2011). Proximal soil sensing: An effective approach for soil measurements in space and time. *Advances in Agronomy*, *113*, 243–291. https://doi.org/10.1016/B978-0-12-386473-4.00005-1

von Hebel, C., Rudolph, S., Mester, A., Huisman, J. A., Kumbhar, P., Vereecken, H., & van der Kruk, J. (2014). Three-dimensional imaging of subsurface structural patterns using quantitative large-scale multiconfiguration electromagnetic induction data. *Water Resources Research*, *50*, 2732–2748. https://doi.org/10.1002/2013WR014864

von Hebel, C., van der Kruk, J., Huisman, J. A., Mester, A., Altdorff, D., Endres, A. L. … Vereecken, H. (2019). Calibration, conversion, and quantitative multi-layer inversion of multi-coil rigid-boom electromagnetic induction data. *Sensors*, *19*(21). https://doi.org/10.3390/s19214753

Waxman, M. H., & Smits, L. J. M. (1968). Electrical conductivities in oil-bearing shaly sands. *Society of Petroleum Engineers Journal*, *8*, 107–122. https://doi.org/10.2118/1863-A

Whalley, W. R., Binley, A., Watts, C. W., Shanahan, P., Dodd, I. C., Ober, E. S., … Hawkesford, M. J. (2017). Methods to estimate changes in soil water for phenotyping root activity in the field. *Plant and Soil*, *415*, 407–422. https://doi.org/10.1007/s11104-016-3161-1

Wunderlich, T., Petersen, H., Attia al Hagrey, S., & Rabbel, W. (2013). Pedophysical models for resistivity and permittivity of partially water-saturated soils. *Vadose Zone Journal*, *12*(4). https://doi.org/10.2136/vzj2013.01.0023

Zhao, P. F., Wang, Y. Q., Yan, S. X., Fan, L. F., Wang, Z. Y., Zhou, Q., … Huang, L. (2019). Electrical imaging of plant root zone: A review. *Computers and Electronics in Agriculture*, *167*. https://doi.org/10.1016/j.compag.2019.105058

How to cite this article: Blanchy G, Watts CW, Richards J, et al. Time-lapse geophysical assessment of agricultural practices on soil moisture dynamics. *Vadose Zone J*. 2020;19:e20080. https://doi.org/10.1002/vzj2.20080